3710–3723 Nucleic Acids Research, 2011, Vol. 39, No. 9 Published online 18 January 2011
doi:10.1093/nar/gkq1325

Species-specific microRNA roles elucidated following astrocyte activation

Eyal Mor[1], Yuval Cabilly[2], Yona Goldshmit[3], Harel Zalts[1], Shira Modai[1], Liat Edry[1], Orna Elroy-Stein[2] and Noam Shomron[1,*]

[1]Department of Cell and Developmental Biology, Sackler Faculty of Medicine, [2]Department of Cell Research and Immunology, George S. Wise Faculty of Life Sciences, Tel Aviv University, Tel Aviv 69978, Israel and [3]Australian Regenerative Medicine Institute, Monash University, Clayton, Victoria 3800, Australia

Received June 2, 2010; Revised and Accepted November 14, 2010

ABSTRACT

MicroRNAs (miRNAs) are short non-coding RNAs that play a central role in regulation of gene expression by binding to target genes. Many miRNAs were associated with the function of the central nervous system (CNS) in health and disease. Astrocytes are the CNS most abundant glia cells, providing support by maintaining homeostasis and by regulating neuronal signaling, survival and synaptic plasticity. Astrocytes play a key role in repair of brain insults, as part of local immune reactivity triggered by inflammatory or pathological conditions. Thus, astrocyte activation, or astrogliosis, is an important outcome of the innate immune response, which can be elicited by endotoxins such as lipopolysaccharide (LPS) and cytokines such as interferon-gamma (IFN-γ). The involvement of miRNAs in inflammation and stress led us to hypothesize that astrogliosis is mediated by miRNA function. In this study, we compared the miRNA regulatory layer expressed in primary cultured astrocyte derived from rodents (mice) and primates (marmosets) brains upon exposure to LPS and IFN-γ. We identified subsets of differentially expressed miRNAs some of which are shared with other immunological related systems while others, surprisingly, are mouse and rat specific. Of interest, these specific miRNAs regulate genes involved in the tumor necrosis factor-alpha (TNF-α) signaling pathway, indicating a miRNA-based species-specific regulation. Our data suggests that miRNA function is more significant in the mechanisms governing astrocyte activation in rodents compared to primates.

INTRODUCTION

Astrocytes, referring to heterogeneous population of cells, are the most abundant glial cells in the central nervous system (CNS). They are involved in a variety of CNS functions as they form structural support to the brain, maintain CNS homeostasis, regulate neuronal signaling, survival and synaptic plasticity by releasing neurotrophic factors and regulating neurotransmitter metabolism. Astrocytes also participate in the formation of the blood–brain barrier (BBB), as they are in juxtaposition to both neurons and blood vessels. The role of astrocytes in local immune reactivity, however, has long been neglected. In response to inflammatory or other pathological conditions, astrocytes leave their quiescent state and become activated. These activated astrocytes are termed reactive astrocytes and the process itself is known as astrogliosis. The purpose of astrogliosis is to contribute to brain repair by isolation of the damaged area and by reconstitution of the BBB. Furthermore, astrogliosis repairs neuron circuits by stimulating axon growth and synaptogenesis in areas distal from the site of initial insult and by forming a non-permissive scar, preventing axon growth into the damaged regions (1). Inflammation can be triggered by signals of bacterial infection such as the endotoxin lipopolysaccharide (LPS) that is found in the outer-membrane of Gram-negative bacteria. LPS was shown to induce the expression and secretion of chemokine and proinflammatory cytokine such as interleukin-6 (IL-6), tumor necrosis factor-α (TNF-α) and interleukin-1β (IL-1β) from astrocytes (2). In the brain, this effect is a global outcome of an intensive cross-talk between astrocytes, microglia and infiltrating peripheral immune cells which interact and facilitate the response in an autocrine/paracrine manner. This results in cytokine and chemokine secretion by astrocytes together with induction of processing and presentation of antigens against Th1, Th2, and naive $CD4^+$ T cells (2,3).

*To whom correspondence should be addressed. Tel: +972 3 6406594; Fax: +972 3 6407387; Email: nshomron@post.tau.ac.il

MicroRNAs (miRNAs) are a group of small (~22 nt) non-coding RNAs that guide post-transcriptional repression of protein-coding genes by base-pairing with the 3′ untranslated region (3′ UTR) of target mRNAs. The miRNA regulatory site is the 'seed' region, comprising bases 2–8 from the miRNA's 5′ end (4), mostly directing full complementation with mRNAs. miRNAs have been extensively investigated in the past few years and over 17 000 miRNAs are now reported, in 142 species, including over 1000 in human [miRBase (5)]. In vertebrates each miRNA is estimated to target several hundred transcripts (6), leading to target mRNA degradation and/or translation inhibition (7), and more than 60% of protein-coding genes are predicted to undergo direct miRNA regulation (8). In some cases, miRNAs were shown to define global tissue-specific mRNA levels (9), while the overall protein output level is consequently adjusted (10,11).

The complexity of brain tissue requires intricate regulation over the expression levels of numerous genes. miRNAs play a significant role in this regulation. Sixty percent of the known miRNAs are expressed in the brain, while some of those enriched or unique for neuronal tissues (12). Most miRNA research of the nervous system has focused on development, in general, or on patterning and cell specification, in particular (13). The most abundant and well-studied CNS miRNA is miR-124 which plays a role in neuronal differentiation (9,14). miRNAs are recognized as vital regulators in immunity and inflammation (15,16). Human astrocyte miRNAs, identified by profiling of multiple sclerosis lesions, include the well-established immune response miRNA—miR-155—which is regulated by several cytokines (17) while the inflammation-associated miR-146a was upregulated in activated astrocytes of temporal lobe epilepsy (TLE) (18).

In the current study, we present a miRNA expression analysis during astrocyte activation by LPS and IFN-γ. The analysis of the differentially expressed miRNAs leads us to subsets of miRNAs, some of which are shared with other immunological related systems in mice and human while others, surprisingly, are mouse and rat-specific. Of special interest are the mouse and rat-specific miR-351 and miR-298, which regulate genes involved in the TNF-α signaling pathway, indicating a miRNA-based species-specific regulation. Altogether, our data suggests that miRNA function holds a more fundamental role in the mechanisms governing astrocyte activation in rodents compared to primates.

MATERIALS AND METHODS

Ethics statement

All experimental procedures involving mice were approved by the Tel Aviv University Animal Care Committee (approval L-07-010). All experiments involving the marmoset monkey were conducted in accordance with the Australian Code of Practice for the Care and Use of Animals for Scientific Purposes and were approved by the Monash University Animal Ethics Committee, which also monitored the welfare of these animals

Preparation of mice primary astrocyte cell culture

Mix glia culture was prepared from the cerebral cortex of 10 C57BL/6 newborn (P1-P3) mice. Cortexes, from which meninges were removed, were collected on ice in HBSS solution (Biological industries, Israel). Following two washes with 20 ml of cold HBSS, cortexes were digested with digestion buffer containing 0.25% trypsin (Sigma, USA) and 100 μg/ml DNase I type IV (Sigma, 1980 KU/mg protein) in Dulbecco's modified Eagle's medium (DMEM; Biological Industries) without serum. More specifically, 5 ml digestion buffer per 10 cortexes was used for two to three times of pipetation followed by addition of 10 ml digestion buffer and incubated for 5 min at room temperature. Fifteen milliliters of cold DMEM containing 10% heat inactivated fetal calf serum (HIFCS) were then added to stop tissue digestion followed by filtration through 100 μm nylon membrane (A.D.Sinon, Israel) into a new 50-ml tube. After centrifugation at 1100 r.p.m. for 10 min at 4°C, the supernatant was aspirated and the cells were resuspended in warm 10 ml DMEM containing 10% HIFCS. Following a second filtration of the cells through 100 μm nylon membrane, the cells were counted in the presence of trypan blue to assess the amount of live cells. Cells were seeded on T75 cm^2 flasks or 150 mm plates pre-coated with 10 μg/ml Poly-L-lysine (Sigma) at a density of $\sim 3.8 \times 10^6$ live cells per flask. The mixed glial cells were incubated in growth medium containing DMEM-10% HIFCS supplemented with 2 mM L-glutamin, 100 U/ml penicillin and 100 μg/ml stretomycin, non-essential amino acids and 110 μg/ml Na-Pyr (all from Biological Industries). The growth medium was replaced at Day 2 and Day 7 after plating. To enrich the mixed glia culture with astrocytes, at Day 13 the flasks were shaken on an orbital shaker at 150 r.p.m. for 18 h, to discard microglia and oligodendrocytes attached at the upper layer of the astrocytes culture. After shaking, the remaining astrocytes were trypsinized and further plated on 10-cm plates at a density of 1×10^6 cells per plate.

Preparation of marmoset primary astrocyte cell culture

Primary astrocyte cultures were derived from the ablated area of PD14 marmoset (*Callithrix jacchus*) primary visual cortex. Meninges were removed and the tissue was mechanically dissociated using a scalpel blade in minimal essential media (MEM) (Gibco, USA). Tissue was then incubated for 20 min in Solution C (476 mg HEPES, 40 mg EDTA, 50 mg trypsin and 2 ml of 1 mg/ml DNase I in 200 ml of calcium and magnesium free heparin-buffered saline solution, adjusted to pH 7.6, filtered-sterilized and stored in −20°C), followed by the addition of an equal volume of Solution A (14 mg of trypsin inhibitor, 1 ml of 1 mg/ml DNase I dissolved in 100 ml MEM, filtered-sterilized and stored in −20°C). After 1 min, the cell suspension was diluted using MEM (1:10), then pelleted, resuspended in DMEM (Gibco) containing 10% FCS, 100 U/ml penicillin and 100 μg/ml streptomycin

and plated into 75 cm flasks (Nunc, Denmark). To enrich the mixed glial culture for astrocytes, flasks were shaken on an orbital shaker at 150 r.p.m. for 4 h. The growth medium was replaced after the shaking process and cells were ready to be used for experiments 1 week later. Primary cultures were trypsinized and re-plated on poly-D-lysine coated chamber slides (Nunc) or into 10-cm Petri dishes (Nunc) at 1×10^4 cells/well or 1×10^6 cells/plate, respectively.

Primary astrocyte cell culture activation and testing

Mice and marmoset astrocytes primary cultures were treated with final concentrations of 2 μg/ml LPS (Sigma, USA) and 3 ng/ml INF-γ (Roche, Switzerland) for 6, 14, 24 and 48 h to induce activation. Enzyme-linked immunoabsorbent assay (ELISA) was performed on medium collected from mice reactive astrocytes according to murine IL-6 and TNF-α ELISA development kit (PeproTech, USA). Recombinant mouse IL-6 and recombinant mouse TNF-α (PeproTech, USA) were used for standard curves.

Cultures purity test by fluorescence-activated cell sorting or immunostaining

Astrocytes were cultured in 10-cm plates and treated as indicated. After incubation, mouse astrocytes were gently removed from the tissue-culture plates by trypsin digestion, then centrifuged at 1100 r.p.m. for 7 min at 4°C. For microglial marker CD11b staining, cells were incubated for 45 min at 4°C in flow cytometry buffer [phosphate-buffered saline (PBS) containing 1% BSA and 0.05% sodium azide] supplemented with PE-conjugated anti-CD11b mAb (BioLegend, USA). For the astrocytic marker GFAP, cells were fixed with cold methanol (–20°C) followed by three washes with flow cytometry buffer and incubation with polyclonal rabbit anti-GFAP ab (DAKO, USA) for 1 h at room temperature. Following three washes with flow cytometry buffer, cells were incubated with anti-rabbit-FITC Fab (Jackson ImmunoResearch, UK). Antigen expression on 5000 live cells was determined by fluorescence-activated cell sorting (FACS) analysis (FACSort; BD Biosciences, USA) and CellQuest software (BD Biosciences).

To confirm marmoset astrocyte culture purity, cell cultured in chamber slides were fixed with 4% PFA for 10 min followed by permeabilization with chilled (–200°C) methanol and blocking with Blocking Solution (PBS containing 2% FCS, 2% GS) for 1 h. Immunostaining was performed using GLAST, early astrocyte marker (1:100, abcam, USA) and CD11b, microglia marker (1:500, Millipore, USA). Cells were incubated with primary antibodies for 2 h, then chamber slides were washed three times in PBS. Cells were then incubated with the secondary antibodies, goat anti-rabbit Alexa594 and goat anti-rat Alexa488 (1:1000, Molecular Probes, USA) for 1 h at room temperature, washed three times in PBS and mounted with Fluoromount (DAKO, USA). The nuclei of cells repopulating the scratched area were visualized by 4′-6-diamidino-2-phenylindole (DAPI) (1:1000; Sigma, USA) staining.

Immunohistochemistry

Sections (40 μm) were examined using standard immunohistochemical procedures to determine expression and localization of microglia marker, CD11d, 3 weeks after brain injury in the marmoset brain (19). Free-floating sections were incubated in PBS containing 0.3% Triton X-100 (PBS-TX) for 1 h, followed by blocking solution [PBS-TX containing 5% normal goat serum (NGS, Invitrogen, USA)] for 1 h at room temperature. Rat anti-CD11b (1:500, Millipore, USA) was diluted in blocking solution and incubated with sections overnight at 4°C. Sections were then washed three times in PBS and incubated with secondary antibody, goat anti-rat conjugated with AlexaFluor 488 (Molecular Probes), for 2 h at room temperature, followed by three 20-min washes with PBS. Sections were then mounted using with Fluoromount (Dako, USA).

RNA extraction

Total RNA was extracted from astrocytes primary cultures or C6 cells using TRIZOL reagent (Invirogen, USA). The final RNA concentration and purity were measured using a NanoDrop ND-1000 spectrophotometer (NanoDrop Technologies, Thermo Scientific, USA).

miRNA profiling

First-strand cDNA was synthesized from total RNA using Megaplex reverse transcriptase reaction with the High Capacity cDNA kit (Applied Biosystems, USA). This reaction contains a specific stem–loop primer for each mature target miRNA. Each stem–loop primer is designed to hybridize to only the fully mature miRNA, and not to precursor forms of its target. The TaqMan Low-Density Arrays (TLDAs) are quantitative real-time-polymerase chain reaction (RT–PCR) assays based on Applied Biosystems technology. The mixture for each sample, containing complementary DNA (cDNA), RNase-free water and TaqMan Universal PCR Master Mix (No AmpErase UNG; Applied Biosystems) was then transferred into a loading port on Rodent TLDA cards A and B, according to the manufacturer's instructions. The card was centrifuged twice, sealed and PCR amplification was carried using ABI Prism 7900HT Sequence Detection System under the following thermal cycler conditions: 2 min at 50°C, 10 min at 95°C, 40 cycles of (30 s at 95°C and 1 min at 60°C). Results were analyzed with SDS software (Applied Biosystems) and the RQ (relative quantity) Manager Software, for automated data analysis. miRNA relative levels were calculated based on the comparative threshold cycle (Ct) method. In short, the Ct for each miRNA and endogenous control snoRNA202 in each sample, were used to create ΔCt values ($Ct_{miRNA} - Ct_{snoRNA202}$). Thereafter, ΔΔCt values were calculated by subtracting the ΔCt of the control untreated astrocytes from the Ct value of astrocytes 48 h following activation. The RQs were calculated using the equation: $RQ = 2^{-\Delta\Delta Ct}$. In addition to *P*-value calculated for the relative levels, we calculated the *P*-value

for the miRNAs raw expression data using unpaired *t*-test and adjusted the values for multiple testing by the false discovery rate (FDR) method of <0.05, (20). Three miRNAs exhibited statistically significant expression increase while one miRNA exhibited statistically significant expression decrease (Figure 2B).

miRNA kinetics by quantitative RT–PCR

First-strand cDNA was synthesized from total RNA using a MultiScribe reverse transcriptase reaction with the High Capacity cDNA kit (Applied Biosystems, USA) and TaqMan MicroRNA Assay RT primer (Applied Biosystems) for each miRNA. Mixtures containing cDNA, RNase-free water, TaqMan Universal PCR Master Mix (No AmpErase UNG; Applied Biosystems) and TaqMan MicroRNA Assay Real-Time probe (Applied Biosystems) for each miRNA were loaded on 96-well plates (Axygen Scientific, USA). PCR amplification and results analysis were done as described under 'miRNA profiling' in 'Materials and Methods' section [Thermal cycler conditions: 2 min at 50°C, 10 min at 95°C, 40 cycles of (15 s at 95°C and 1 min at 60°C)], while 6, 14, 24 and 48 h of activation were compared to untreated astrocytes to yield the RQ.

mRNA kinetics by quantitative RT–PCR

First-strand cDNA was synthesized from total RNA using a MultiScribe reverse transcriptase reaction with the High Capacity cDNA kit (Applied Biosystems, USA) and random hexamer primers (Applied Biosystems). Mixtures containing cDNA, RNase-free water, specific primers (see 'Primers' in 'Materials and Methods' section) (Sigma, USA) and Power SYBR green PCR master mix (Applied Biosystems), were loaded on 96-well plates (Axygen Scientific, USA). PCR amplification was done as described under 'miRNA profiling' in 'Materials and Methods' section (Thermal cycler conditions: 2 min at 50°C, 10 min at 95°C, 40 cycles of (15 s at 95°C and 1 min at 60°C) and dissociation curve cycle of 15 s at 95°C, 15 s at 60°C and 15 s at 95°C. The dissociation curve is required to show a united peak for all samples, meaning that only one product was created. Standard curve was first created for each pair of primers to determine proper primer concentration for linear amplification. Results' analysis was done as described under 'miRNA profiling' in 'Materials and Methods' section, using GAPDH as endogenous control.

PCR primers

miRNA cluster: (i) miR-503-Fwd: CCT AGC AGC GGG AAC AGT AC, miR-351-Rev: TAA CAC TCT TCT CCA GTT CCC; (ii) miR-322-Fwd: GAA GGG CTG CAG CAG CAA TT, miR-503-Rev: TAC TCC AGG GCA CCA AAC AC. Mice gene qPCR: GAPDH-Fwd: TGC ACC ACC AAC TGC TTA G, GAPDH-Rev: GGA TGC AGG GAT GAT GTT C; PEA15-Fwd: TAC AGA ACC CGT GTG CTG AA, PEA15-Rev: GGC TGC CGG ATA ATG TCT TT; TNF-α-Fwd: TGT AGC CCA CGT CGT AGC, TNF-α-Rev: TTG AGA TCC ATG CCG TTG G; SIAH2-Fwd: ATG CCG CCA GAA GTT AAG C, SIAH2-Rev: AGC CCG TGG TAG CAT ACT TA. Marmoset gene qPCR: GAPDH-Fwd: AAA GTG GAT GTC GTC GCC ATC AAT GAT, GAPDA-Rev: CTG GAA GAT GGT GAT GGG ATT TCC ATT; TNF-α-Fwd: CAG CCT CTT CTC CTT CCT GCT, TNF-α-Rev: GCC AGA GGG CTG ATT AGA GA; SIAH2-Fwd: GGC AGT CCT GTT TCC CTG TA, SIAH2-Rev: CAC TTG CAG GAA GCA CCA G; C6 cells (rat) gene qPCR: GAPDH: as in mice. TNF-α-Fwd: GCC TCT TCT CAT TCC TGC TC, TNF-α-Rev: GAG CCC ATT TGG GAA CTT CT; SIAH2-Fwd: ATG CCG CCA GAA GTT GAG C, SIAH2-Rev: AGC CCG TGG TGG CAT ACT TA.

3′ UTR constructs

Fragments of 700 bp of TNF-α, 500 bp of SIAH2 and 400 bp of PEA15 3′ UTR spanning the miRNAs binding sites were cloned into the XhoI–NotI restriction site downstream to the Renilla Luciferase Reporter of the psiCHECK™-2 plasmid (Promega, USA) that contain a Firefly Luciferase Reporter (used as control) under a different promoter. For this purpose, the 3′ UTR fragments were PCR-amplified from mice brain cDNA and XhoI–NotI restriction sites were added (italics), using the primers: TNF-α-Fwd: ACA *CTC GAG* CCC TTT ATT GTC TAC TCC TCA; TNF-α-Rev: AAG GTC AA*G CGG CCG C*CA ATG ACC CGT AGG GCG ATT; SIAH2-Fwd: ACA *CTC GAG* TCG GTG ATC TCA AAA TCA ACT C; SIAH2-Rev: AAG GTC AA*G CGG CCG C*CA AGG GAA GCC ATA TGT AAA C; PEA15-Fwd: ACA *CTC GAG* CGT GCT AAC TGT GTG TGT ACA T; PEA15-Rev: AAG GTC AA*G CGG CCG C*AA GGC AGG TGT CTG CAG CA; The miRNA-binding sites were site-directed mutated by PCR reaction of the plasmid using the enzyme PfuUltra II Fusion HS DNA Polymerase (Genex, USA), and the PCR reaction: (i) 95°C for 2°min, (ii) (95°C for 20 s, 58°C for 20 s, 72°C for 2 min) X16, (iii) 72°C for 3 min. The primers used for mutagenesis were the ones indicated below (target nucleotides in italics) and complementary Reverse primers: TNF-α-351-(miR-351 binding site)-Fwd: AGG GGA TTA TGG CTC *CTA T*TC AAC TCT GTG CTC; TNF-α-298-Fwd: TAC ATC ACT GAA CCT *AAC A*TC CCC ACG GGA GCC G; SIAH2-351-Fwd: CTT GAC AGA TCG CTC *CTA T*CT GCC TCC CCC TGC C; SIAH2-298-Fwd: GCT TTA AGG CGT CCT *AAC A*TG ACA CTG TTG GTC T; PEA15-155-Fwd: TTT GTG GTT TTT AGC *CGC G*AC TTA TTG TCT AGG C. Products were then incubated with DPN1 (New England BioLabs, UK) that digest the methylated source plasmid and the mutated plasmid was sequenced.

miRNA constructs

Pre-miRNAs were cloned into the BamI–EcoRI restriction site of the miRNA expression vector miRVec that was provided by Prof. R. Agami (21). For this purpose, the genomic loci of ~200 bp upstream and downstream of the pre-miRNAs was PCR-amplified from mice tail

gDNA or HeLa cells (for miR-155) and BamI–EcoRI restriction sites were added (italics), using the primers: miR-351-Fwd: *GCG GAT CC*A GGT GGT ACA ATG AGA GGC A; miR-351-Rev: *GCG AAT TC*A GGC CTC CTC TAA CTG TAC C; miR-298-Fwd: *GCG GAT CC*C TCTT TGT GCT ACT ACA TG; miR-298-Rev: *GCG AAT TC*C ACT GCA TCG ACA ATG GGA A; miR-155-Fwd: *GCG GAT CCG* GAT TTA ATG AGC TCC TTC CTT TCA AC; miR-155-Rev: *GCG AAT TC*C TAA ATG CAA ACA TTT TCA TTT AAA TG.

Dual Luciferase assay

HEK293 cells were seeded in 24-well plates in DMEM supplemented with 10% FBS and 1% Pen/Strep. Cells were transfected using theTransIT-LT1 Transfection Reagent (Mirus, USA), according to the manufacturer's instructions, with 500 ng DNA: 5 ng psiCHECK™-2 containing the desired 3′ UTR with or without site-directed mutations; 10 ng GFP vector and 485 ng miRVec containing the desired pre-miRNA or an empty vector. Forty-eight hours after transfection, the transfection efficiency was measured by green fluorescent protein (GFP) fluorescence, indicating a transfection efficiency of ~50% repeatedly, and firefly and Renilla Luciferase activities were measured using the Dual-Luciferase Reporter Assay System kit (Promega, USA) and a Veritas microplate luminometer (Promega), according to Promega's instructions.

C6 astrocytoma cells activation and miRNA manipulation

C6 cells were seeded in six-well plates in DMEM supplemented with 10% FBS and 1% Pen/Strep. Transfections were done using Lipofectamine 2000 transfection reagent (Invitrogen, USA) according to the manufacturer's instructions. Transfection efficiencies were measured by GFP fluorescence in C6 cells, indicating a transfection efficiency of ~50% repeatedly. For activation, 24 h after seeding, cells were starved from FBS for 12 h prior to treatment with LPS (2 μg/ml) and IFN-γ (3 ng/ml) for 18 h. For miRNA over-expression, 24 h after seeding, transfection was done with 2.5 ug miRVec containing the desire pre-miRNA (or an empty vector). Cells were either taken for RNA purification after 27 h or were starved after 21 h following by activation for 18 h. For miRNA inhibition, transfection was done with 70 pmol Anti-miR miRNA Inhibitors or a scrambled inhibitor (Ambion Applied Biosystems, USA). Cells were taken for RNA purification 24 h later.

Statistics

P-values were calculated using a paired/unpaired *t*-test or Chi-square test.

RESULTS

The involvement of miRNAs in astrocyte activation

Several studies have addressed the changes in gene expression following activation of astrocytes with LPS and/or INF-γ (22–24). To address the issue of miRNAs involvement in regulation of gene expression during astrocyte activation, we isolated astrocytic cells from cerebral cortex of newborn C57BL/6 mice, and exposed the primary cultures to LPS and INF-γ (see 'Materials and Methods' section). The purity of the cultures was determined by flow cytometry analysis that showed over 90% GFAP-positive cells (and ~95% CD11b-negative cells), representing astrocytes (Supplementary Figure 1). The activation process was accompanied by a steady increase in secretion of interleukin 6 (IL-6) and TNF-α as measured in the medium at 6–48 h following LPS and INF-γ application (Figure 1), consistent with previous reports (2,25). In an effort to understand the complete network of gene interactions during astrocyte activation, we performed global analysis of miRNA expression in astrocytes treated with LPS and INF-γ for 48 h compared to untreated astrocytes (The full table is available in Supplementary Table 1). We found that resting astrocytes highly express a set of miRNAs, among which are miR-26a and miR-29a, previously shown to be abundant in this cell type (26) (Supplementary Table 2). Analysis of the differentially expressed miRNAs in treated and untreated astrocytes revealed a significant alteration in the expression levels of several miRNAs, enabling the definition of a distinct miRNA expression signature upon LPS and INF-γ-induced activation (Figure 2). This observation suggests that some miRNAs play a role in the gene regulatory networks following astrocyte activation.

The mouse and rat-specific miR-351 is transcribed as part of a conserved miRNA cluster

In any given cellular process, out of the entire miRNA repertoire, usually only a few miRNAs show differential expression. Similarly, in our experiments, most miRNAs did not exhibit differential expression in treated versus non-treated astrocytes (Figure 2A). However, 12 miRNAs exhibited increased expression of more than 2-fold following activation ($P < 0.033$) while the expression of six miRNAs decreased more than 3-fold ($P < 0.01$). These miRNAs were considered for further analysis (see 'Materials and Methods' section for further statistical analysis by false discovery rate). Selected miRNAs are presented in Figure 2B. Among the upregulated miRNAs, we observed several, including miR-155, miR-146a/b and

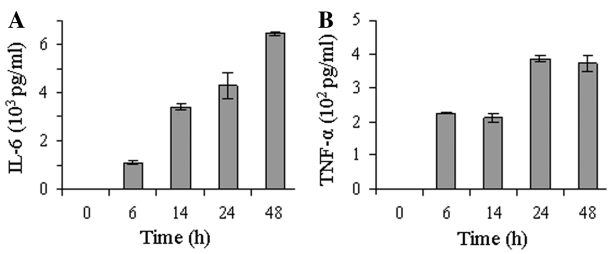

Figure 1. Astrocyte activation by LPS and IFN-γ. IL-6 (**A**) and TNF-α (**B**) secretion into the medium detected by ELISA following 6 h, 14 h, 24 h and 48 h of LPS (2 μg/ml) and IFN-γ (3 ng/ml) treatment of mice astrocytes demonstrates the biological activity of astrogliosis. Note that neither IL-6 (A) nor TNF-α (B) cytokines were secreted from untreated astrocytes, while their secretion was dramatically increased during the LPS and INF-γ treatment. Values represent mean levels ± SEM ($N = 4$). $P < 2e\text{-}05$ for all bars compared to untreated astrocytes.

Table 1. Selected miRNAs modified expression in diverse LPS/IFN-γ-treated systems and in our experiments

miRNA	Organism	Activation system	Direction	Time[a] (h)	Ref.	Astrocytes RQ[b] – our study
miR-146a	Human	Monocytes (LPS)	Activation	8	(63,64)	14.4
miR-155	Mouse	Macrophages (LPS)	Activation	48	(65)	13.2
	Human	Monocytes (LPS)	Activation	8	(63,64)	13.2
	Mouse	Macrophages (IFN-γ)	Activation	24	(66)	13.2
miR-146b	Human	Monocytes (LPS)	Activation	8	(63,64)	8.0
	Human	Leukocytes (*in vivo*, LPS)	Suppression	4	(67)	8.0
miR-147	Mouse	Macrophages (LPS)	Activation	24	(68)	5.7
miR-222	Human	Monocytes (LPS)	Activation	8	(64)	2.2
miR-142-3p	Mouse	Lungs (*in vivo*, LPS)	Activation	6	(69)	2.2

[a]Latest time tested in which the observed expression was apparent.
[b]Relative Quantification ($2^{-\Delta\Delta ct}$) from our experiments compared to small RNA control and untreated astrocytes ($N = 3$, $P < 0.033$).

miR-147, that were previously shown to be induced in diverse immunological-related cellular systems, such as monocytes and macrophages, upon LPS or IFN-γ treatment (Table 1; and references within). This indicates a global inter-cellular response among astrocytes and immune cells. Interestingly, two of the mostly suppressed miRNAs in reactive astrocytes, miR-351 and miR-298, are reported to be specific to mice and rats (see miRbase: http://www.mirbase.org). The miR-351 gene is found only in mice and rats (Figure 3A). Additional miRNA gene identifying algorithms could not locate miR-351 gene in any other animal (see miRNAminer: http://groups.csail.mit.edu/pag/mirnaminer and miRviewer: http://people.csail.mit.edu/artzi/miRviewer). miR-351 belongs to the miR-125 family, shown to perform varied roles in development, cancer and inflammation (27–30) (Figure 3B). Members of a miRNA family share the regulatory 'seed' region, dictating their targeting. The fact that some members of the miR-125 family potentially regulate the same target genes while they are species specific raises the question if these miRNA genes evolved independently to take up species-specific functions. To address this question, we chose to compare miR-351 to other members of the miR-125 family on the level of: (i) genomic loci; (ii) expression levels; and (iii) gene targets. In mice and rats, miR-351 resides within a well-conserved miRNA cluster (Figure 3C). It appears that all the expressed miRNAs in this cluster are downregulated 48 h following astrocyte activation, suggesting that they are all controlled under a common transcriptional unit (Figure 3C). Using primers complementary to the pre-miRNAs sequences of the mice miR-351, miR-503 and miR-322, we could amplify by RT–PCR the region transcribed upstream to miR-351 and thus confirmed that miR-351 is transcribed into a large transcript which can harbor at least part of the miRNA cluster (Figure 3D). For comparison, other members of the miR-125 family in mice are located either solely in introns (miR-125b-1 and -2) or in a miRNA cluster (miR-125a; together with miR-99b and let-7e). The second mouse and rat-specific miRNA, miR-298, possesses a different mature sequence in mice and rats, including the seed region, compared to that of primates (Figure 3A). For this reason miR-298 is hereafter termed miR-298.mr to indicate its mouse and rat-specific seed region [as in TargetScan (8)]. As a consequence, this miRNA targets a different set of genes in mice and rats compared to primates, thus probably having a different regulatory function. We note that this assumption is based on 'seed'-related computational predictions only (31–34) while other targeting rules exist (35).

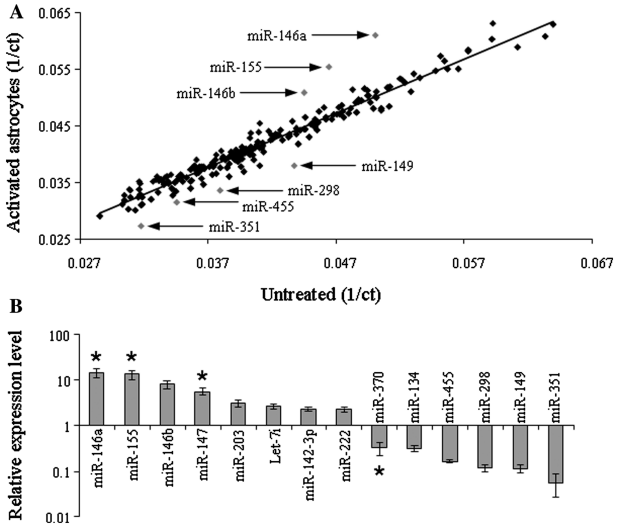

Figure 2. miRNA expression signature following astrocyte activation in mice. Mice cortical astrocytes primary cultures were incubated with LPS and IFN-γ (2 μg/ml and 3 ng/ml, respectively). Following 48 h total RNA was purified and miRNA levels were assayed on a high-throughput quantitative real-time PCR array. (**A**) Scatter-plot representation of the distribution of miRNAs expressed in treated astrocytes compared with those from untreated cultures. Values are presented as 1/threshold-cycle (1/ct) mean ($N = 3$). miRNAs with $ct \geq 40$ (0.025 on this graph) were not taken into consideration. miRNAs that are deviating from the linear regression line by at least 15% (up) or 8% (down) are indicated. (**B**) Relative Quantification (RQ) ($Log(2^{-\Delta\Delta ct})$) of selected miRNAs. Comparison was made to a non-related small non-coding RNA (snoRNA202) and to untreated astrocytes. Values are presented as mean ± SEM ($N = 3$, each repeat containing a mixture of at least two independent cultures, $P < 0.033$). miRNAs with a statistically significant differential expression (unpaired *t*-test adjusted for multiple testing by FDR of <0.05, see 'Materials and Methods' section) are marked with an asterisk.

miR-351 and miR-125b expression levels are complementary in rodents and primates

Activation of macrophages and dendritic cells via exposure to LPS and IFN-γ elicits an innate immune

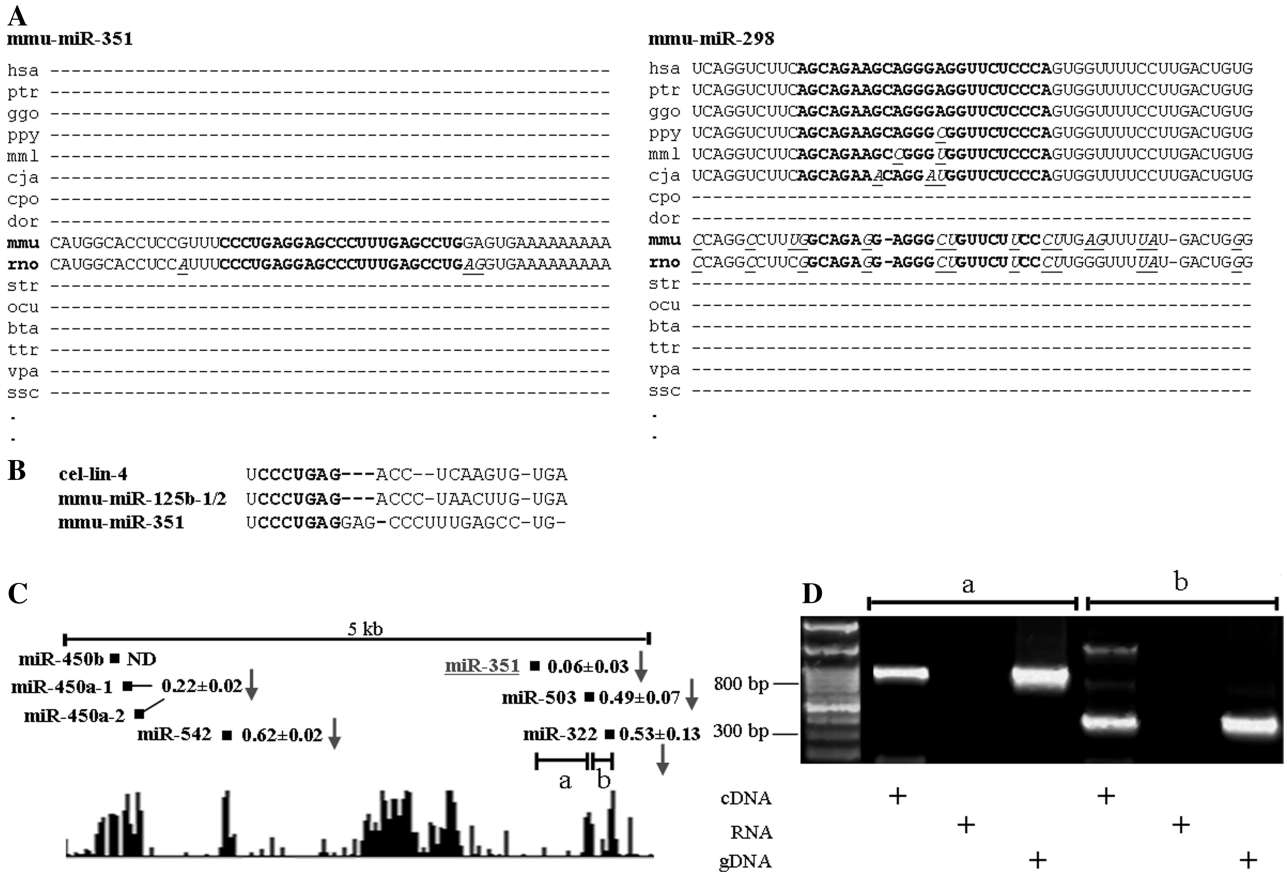

Figure 3. The evolution of miR-351 and miR-298.mr. (**A**) Evolutionary conservation of miR-351 and miR-298. Images are reproduced from miRviewer (http://people.csail.mit.edu/artzi/miRviewer). miR-351 and miR-298.mr are unique to mice (mmu – *Mus musculus*) and rats (rno – *Rattus norvegicus*). Bolded nucleotides represent the mature miRNA. Nucleotide variations are italicized and underlined. (**B**) Alignment of mature miRNA sequences from the miR-125 family (cel – *Caenorhabditis elegans*). Bolded nucleotides represent the regulatory 'seed' region which is identical to all family members. (**C**) An on-scale representative of the genomic locus of the mouse miR-351 gene. Arrows indicate downregulation of the miRNA expression level 48 h following activation to the level indicated (mean ± SEM, $N = 3$). miR-450a-1 and 2 could not be distinguished. ND – not detected. All miRNAs genes in this cluster, except for miR-351 gene are evolutionarily highly conserved as can be seen in the conservation plot below (reproduced from UCSC Genome Browser). (**D**) Reverse transcription PCR of the RNA transcript precursor of miR-351. Using primers complementary to the pre-miRNAs sequences of the mice miR-351, miR-503 and miR-322 that were designed to amplify the regions indicated in (C), we observed that miR-351 gene is transcribed in a single transcriptional unit together with miR-503 (a) which is transcribed together with miR-322 (b). Bands can be observed in cDNA and genomic DNA (gDNA) amplification but not in RNA (to exclude gDNA contamination).

response which is accompanied with a significant change in gene expression (36,37). We have shown that miRNA expression is changed under similar conditions in brain astrocytes as well. Assuming that this response is conserved among various organisms, it was surprising that miR-351 and miR-298.mr, tagged as possible important regulators, were found to be species specific. We hypothesized that if miR-351 was indeed functional then its expression level would mimic that of its other family members from different organisms. To test this hypothesis, we compared the expression pattern of the miRNAs mostly altered in our data in mice and primates following astrocyte activation. For this purpose, we generated primary astrocyte cultures from visual cortex of PD14 marmoset (*C. jacchus*). The marmoset astrocyte cultures' purity was determined by Immunostaining with the microglia marker CD11b and the astrocyte marker GLAST (38) that showed a total purity for astrocytes (Supplementary Figure 2A). LPS- and INF-γ-induced activation in these cultures was accompanied by induction of IL-6 and TNF-α mRNA levels (Supplementary Figure 2B). Following treatment of the mice and marmoset astrocytes with LPS and INF-γ, we monitored the expression level of the miRNAs along a continuous time course. The expression level of the conserved miRNAs, miR-155 and miR-146a, gradually increased in both species from 6 through 14 and 24 h after treatment, reaching their maximum levels at 48 h (Figure 4). While miR-155 upregulation was more prominent in mice, miR-146a upregulation was stronger in marmoset. The expression of other conserved miRNAs, miR-149 and miR-455, gradually decreased in both mice and marmoset while, interestingly, the expression of the mouse and rat-specific miR-298.mr was also gradually downregulated. The expression of the second mouse and rat-specific miRNA, miR-351, was downregulated in mice (reduced by 54% at 24 h after treatment), similarly to its family member miR-125b, which was downregulated in marmoset (by

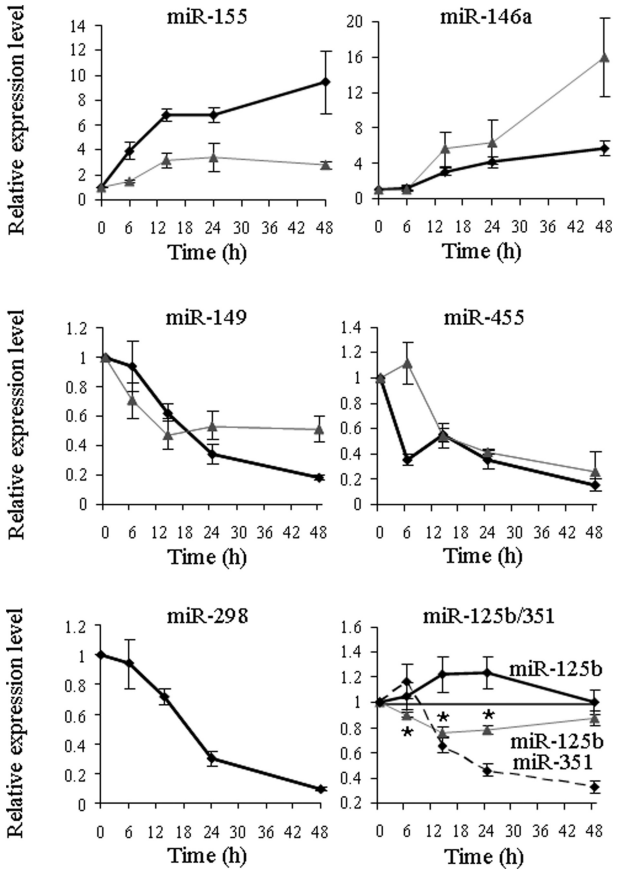

Figure 4. Mice and monkey miRNAs expression following astrocyte activation by LPS and INF-γ. Astrocytes primary cultures from mice and marmoset were incubated with LPS and IFN-γ for 6, 14, 24 and 48 h. The RNA was purified and miRNA levels were measured by quantitative real-time PCR. Black/gray plots represent mice/marmoset miRNAs, respectively. miR-351 plot is dashed. Values are presented as miRNA Relative Quantification ($2^{-\Delta\Delta ct}$) levels compared to non-coding RNA control (snoRNA202) and untreated astrocytes. Values are presented as mean ± SEM ($N = 4$). Marmoset miR-125b expression is marked by asterisk where $P < 0.03$.

22% at 24 h, $P < 0.03$). Note that the expression of miR-125b did not significantly change in mice, whereas miR-351 does not exist in marmoset. Given that miR-125b was implicated in other inflammatory systems such as macrophage activation (28,39,40), skin inflammation (41) and, recently, IL-6-induced astrocyte activation (42), these data suggest that miR-351 in rodents may have some overlapping regulatory roles to miR-125b in primates. Taken together, these results implicate that the mice and rat-specific miR-351 and miR-298.mr may have a functional significance during astrocyte activation and that miR-351 might have overtaken miR-125b roles.

Mouse and rat-specific miRNAs target genes associated with the TNF-α signaling pathway

miRNAs exert their effect by binding to mRNA sequences. The most common mode of target identification is based on sequence complementary and target site conservation. We employed one such tool, TatgetScan (8), for predicting targets of the miRNAs that were most significantly changed after activation. Given that the TNF-α signaling pathway is a major player in immune responses as well as in CNS diseases we first asked whether this pathway can be targeted by miRNAs in activated astrocytes. We searched for targets of miR-155 that are decreased in mice activated astrocytes and that were previously shown to regulate TNF-α signaling pathway. PEA15, that diverts astrocytes from TNF-α-triggered apoptosis by regulating ERK/MAPK cascade action and blocking caspase recruitment by FADD (43,44), was among TNF-α-related genes predicted with high confidence to be regulated by miR-155. PEA15 mRNA expression kinetics was inversely correlated to that of miR-155, suggesting an inhibitory regulatory relationship with this miRNA (Figure 5A).

Given that miR-351 and miR-298.mr are specific to mice and rats, we screened the predicted target genes of either of these miRNAs to the ones possessing the miRNA-binding site in both mice and rats. Interestingly, miR-351 and miR-298.mr have more common targets than expected by chance (312, 253, respectively, $P = 1.7E\text{-}54$, χ^2-test), which may suggest a common regulatory function for these miRNAs. Such a significant phenomenon was also apparent in a conservative method of looking at evolutionary conserved targets only (22 common targets, 10 expected, $P = 4E\text{-}4$, Chi-square test). This common target gene list is highly enriched with brain over-expressed genes [~60%, $P = 5E\text{-}16$, 'UP_Tissue', DAVID Bioinformatics Resources (45)], suggesting that the common function of miR-351 and miR-298.mr is predominantly in the brain.

We searched for miR-351 and miR-298.mr common targets that are known to regulate TNF-α signaling pathway. Among these, we found TNF-α itself. This gene 3′-UTR possesses three evolutionary conserved binding sites for miRNAs regulated by >2.5-fold 48 h following astrocyte activation. Remarkably, these three miRNAs, miR-351, miR-298.mr and miR-149, are the three most downregulated miRNAs in mice astrocyte activation according to our expression profiling (Figure 2). As mentioned, miR-298.mr and miR-351 are mouse and rat-specific and while the TNF-α 3′ UTR binding site for miR-298.mr is conserved among most species, miR-351/125b binding site is found in mice but not in primates or rats so the parallel downregulation of miR-125b in marmoset will have no effect on TNF-α. Thus, TNF-α is predicted to be regulated by miRNAs profoundly in mice and rats astrocytes, which may be attributed to keeping TNF-α mRNA increase following mice astrocyte activation compared to marmoset (~55-fold and ~1-fold, respectively, 14 h following activation) (Figure 5A).

Among predicted targets of both miR-351 and miR-298.mr the E3 ubiquitin–protein ligase SIAH2 (seven in absentia 2) stands out. SIAH2 mediates TNF-α-induced ubiquitylation and degradation of TRAF2 (46). Similar to the TNF-α 3′ UTR, SIAH2 binding site for miR-298.mr is conserved among most species while miR-351/125b binding site is not found in primates. This suggests that the TNF-α signaling pathway may be profoundly regulated by miRNAs in mice and rats

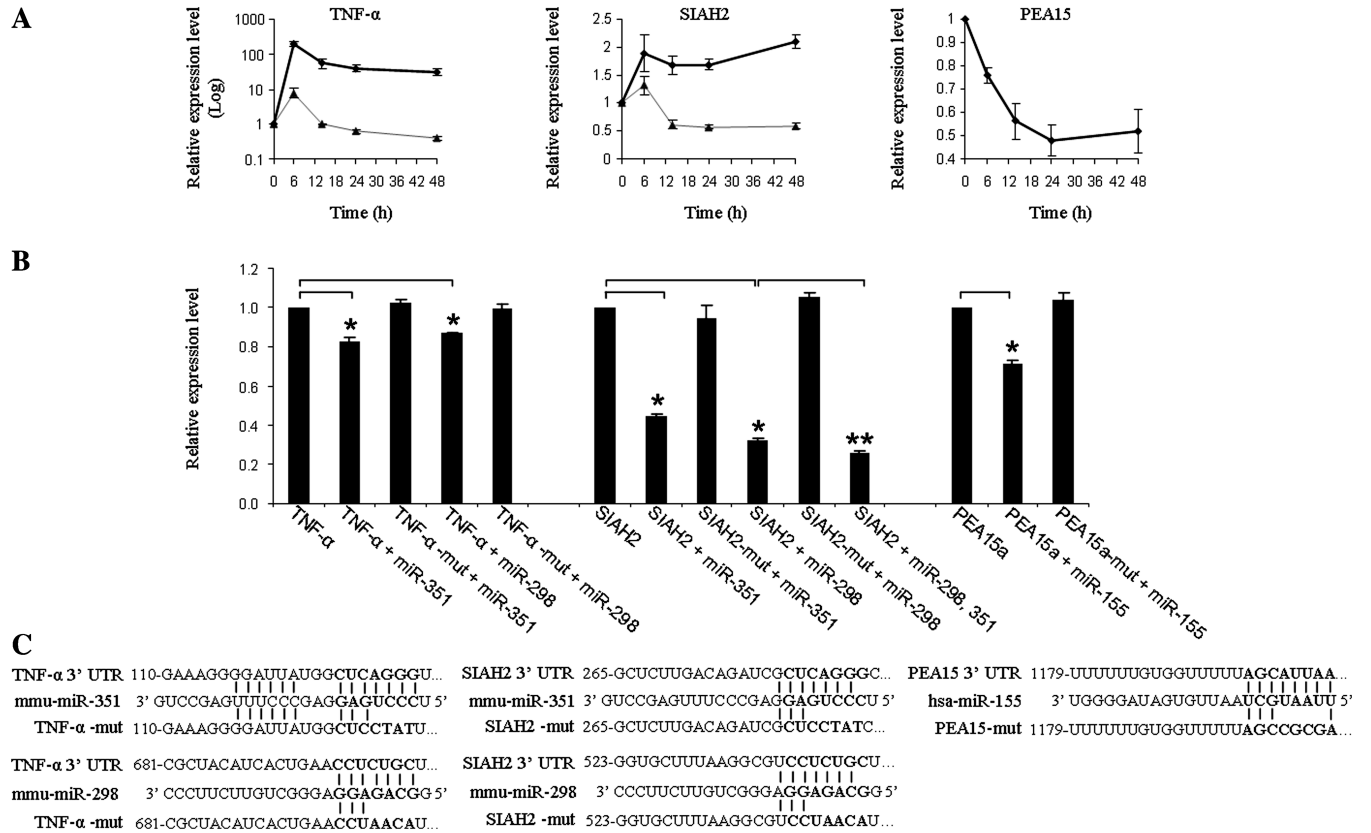

Figure 5. TNF-α signaling pathway related genes 3′-UTRs are modulated by miRNAs. (**A**) Astrocytes primary cultures were incubated with LPS and IFN-γ for 6, 14, 24 and 48 h. Following RNA purification mRNA levels were measured by quantitative real-time PCR. Values are presented as levels of mRNA relative quantification ($2^{-\Delta\Delta ct}$), or [Log($2^{-\Delta\Delta ct}$)], compared to controls (GAPDH) and untreated astrocytes, as mean ± SEM ($N = 4$). Black/gray plots represent mice/marmoset mRNA, respectively. (**B**) Predicted targets 3′-UTRs spanning miRNAs binding sites were cloned to the psiCHECK-2 plasmid downstream to a Renilla luciferase reporter gene. This plasmid (or its mutated version) was cotransfected along with a plasmid containing the correlated pre-miRNA to HEK293 cells. Renilla luciferase activity was measured 48 h following transfections and normalized to Firefly luciferase activity and transfections with control plasmid instead of a miRNA. Values are presented as mean ± SEM ($N > 3$) with a $P < 0.003$ (single asterisk) or 0.03 (double asterisk). (**C**) Representation of miRNA–mRNA interactions tested in the Luciferase assay, including the mutations generated in the miRNA-binding sites.

astrocytes, through TRAF2 stabilization. This SIAH2 regulation by miRNAs may be attributed to maintaining SIAH2 mRNA at high levels following mice astrocyte activation compared to marmoset (~1.7- and ~0.6-fold, respectively, 14 h following activation) (Figure 5).

In order to validate these miRNA predicted targets, we first tested the direct interaction for the miRNA-target pairs. We employed the Luciferase reporter assay. Target genes 3′-UTRs spanning the miRNA-binding sites were cloned downstream to a Renilla Luciferase reporter gene. Reporter plasmids and miRNAs were cotransfected into HEK293 cells. Relative expression of the Renilla Luciferase reporter was measured compared to a Firefly Luciferase reporter, a control transfection and the 3′UTRs mutated in the miRNA binding site (see 'Materials and Methods' section and Figure 5C). Both miR-351 and miR-298.mr significantly reduced the Renilla Luciferase-TNF-α activity to 82–87% compared to a control plasmid (Figure 5B). Similar results were obtained when using SIAH2 3′UTR but to a larger extent: both miR-351 and miR-298.mr reduced the Luciferase activity to 32–44%. Interestingly, when cotransfecting the two miRNAs together (the total amount of the miRNAs was maintained at constant levels), a larger reduction of the Luciferase activity was observed. This suggests a synergistic function of miR-351 and miR-298.mr when regulating SIAH2. Similarly, PEA15 3′ UTR was affected by miR-155.

In order to further test miR-351 and miR-298.mr regulation upon TNF-α and SIAH2 in astrocyte activation, we employed the rat astrocytoma C6 cell line, which is used as a model of astrocytes and their activation (e.g., see refs. 47 and 48). Since C6 are rat derived cells, while our primary cultures are mouse-derived, we should note that TNF-α 3′-UTR possesses a binding site for miR-298.mr and miR-351 in mice but only for miR-298.mr in rats. SIAH2 possesses binding sites for both miRNAs in mice and rats. We first activated C6 cells with the same levels of LPS and INF-γ that were used for the primary cultures (see 'Materials and Methods' section and ref. 49). The activation was accompanied with TNF-α increase and with miR-351 and miR-298.mr decrease in accordance with activation of mice cultured astrocytes (Figure 6A). We then over-expressed miR-298.mr prior to activation

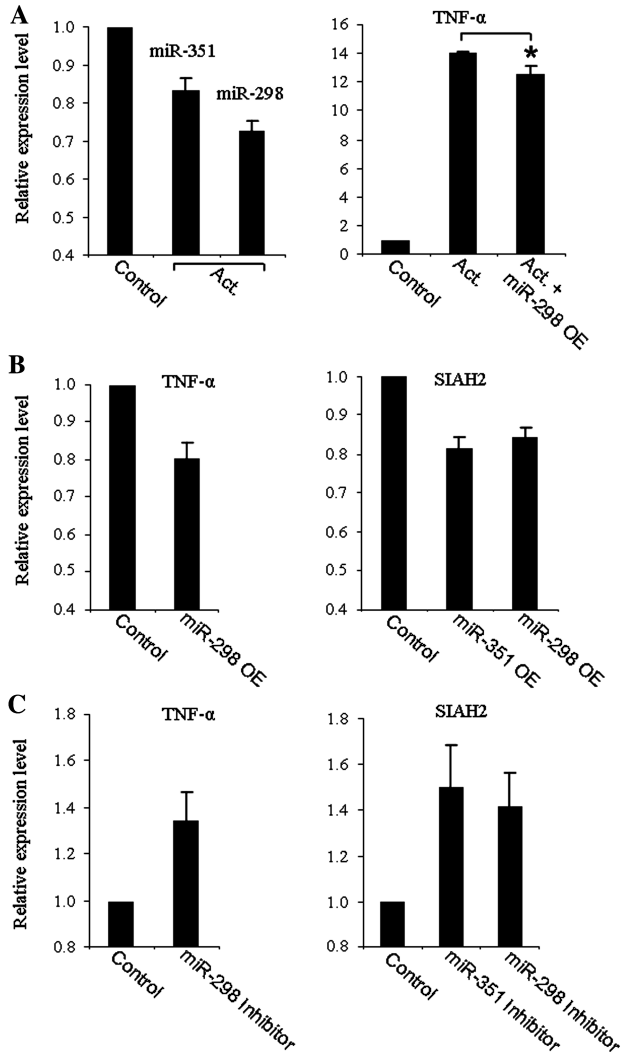

Figure 6. TNF-α and SIAH2 expression is regulated by miR-351 and miR-298.mr in C6 astrocytoma cells. (**A**) C6 cells were treated with 2 μg/ml LPS and 3 ng/ml INF-γ for 18 h (Act., Activation) with or without initial over-expression (OE) of miR-298.mr (or a control plasmid). Following RNA purification, miRNA or mRNA levels were measured by quantitative real-time PCR. Values are presented as levels of relative quantification ($2^{-\Delta\Delta ct}$) compared to controls (non-coding RNA snoRNA202 or GAPDH) and non-activated cells. (**B**) miR-351 and miR-298.mr were over-expressed in C6 cells for 27 h. mRNA levels were measured as in (A). Control wells were transfected with an empty vector control plasmid. (**C**) miR-351 and miR-298.mr expression was inhibited in C6 cells for 24 h. mRNA levels were measured as in (A). Control wells were transfected with a scrambled inhibitor. All values are presented as mean ± SEM ($N \geq 3$) with a $P < 0.05$ (asterisk).

which resulted in a reduction of TNF-α increase. miR-298.mr and miR-351 over-expression prior to activation also reduced SIAH2 levels (Supplementary Figure S3). In addition, TNF-α was reduced by over-expression of miR-298.mr without activation, while SIAH2 levels were reduced by both miRNAs in the same conditions (Figure 6B). Finally we inhibited miR-298.mr and miR-351 endogenous expression levels (between 26% and 35%) resulting in TNF-α (by miR-298.mr inhibition) and SIAH2 (by both miRNA inhibition) increase (Figure 6C). Altogether, we have shown that key miRNAs in activated astrocytes, specific to mouse and rat, target genes associated with the TNF-α signaling pathway.

DISCUSSION

A controlled reaction to trauma has proven fundamental for the CNS (25). Given that astrocytes are vital players in brain homeostasis, it is of importance to understand the involvement of miRNAs in their activation which may lead to enhanced CNS recovery. In this work, we have demonstrated a global shift in miRNA expression in astrocytes treated with LPS and IFN-γ. Among the significantly altered miRNAs, several possess key roles in the response of immunological systems such as monocytes and macrophages to bacterial and/or cytokine stimulation (Table 1), thus suggesting that cellular pathways common for astrocytes and cells of the immune system are actively monitored by overlapping miRNA regulation.

We found that two of the most downregulated miRNAs following astrocyte activation in mice are found in mouse and rat species exclusively, implying a unique mode of regulation for these species in CNS innate immunity. The miR-351 gene was shown to be involved in immune responses as it is able to attenuate viral replication (50) while its family member, the primate miR-125b is induced by IL-6 in human astrocytes (42), contradicting its repression by LPS and IFN-γ. The mouse and rat version of miR-298 was shown to be upregulated in the hippocampus and blood of rats with ischemic stroke, intracerebral hemorrhage and kainate seizures (51) as well as in rat brains of transient focal ischemia (52). The caveat of these studies is in their heterogeneous cell population. We, on the other hand, show a strong reduction of miR-298.mr in purified mice activated astrocytes. Other studies addressed miR-298.mr function (53,54), yet none have addressed its diverse function in different species.

We have generated a list of all mouse and rat-specific miRNAs (37 in total, Supplementary Table S3). The genes of 36 out of these are found in mice and rats only (including miR-351), while miR-298.mr has undergone mutations in the seed region, thus very likely altering its target gene pool (mirBase, miRviewer and TargetScan). While mRNAs are under selective pressure to maintain 7-nt sites matching miRNAs (55), miRNA predicted gene targets are considered more reliable when the miRNA-binding site is evolutionary conserved and thus can be predicted above the background of false-positive predictions (8). The upper 10 percentiles of miRNAs have more than 450 predicted targets with conserved binding sites (6), while mouse and rat-specific miRNAs have a relatively low number of these (201, TargetScan). This is not surprising given an ancient co-evolution for conserved miRNAs and their targets (6) and the lack of such a process in the case of species-specific emergence of a miRNA. Thus, evolutionary conserved miRNAs may have developed more prominent regulatory roles and have attracted much more attention so far compared to very few studies addressing species-specific miRNAs. miR-351, however, stands out as having many conserved

targets (519), belonging to a group of only four mouse and rat-specific miRNAs (including miR-291a-3p, miR-294 and miR-295), which have 3.1-fold more conserved targets than the average of their type ($P = 1.0E-4$ according to TargetScan, Figure 7A and Supplementary Table 3). Each of these four miRNAs is part of a conserved miRNA family in which all members share their functional seed region and thus gene targets. miR-351 belongs to the miR-125 family which originates at the first identified miRNA, lin-4 (56). Thus, miR-351 may regulate the genes that have developed as targets for other more ancient family members and thus seem to hold prominent roles in mice and rats (Figure 7B). miR-298.mr does not belong to a miRNA family, yet we notice that the region spanning its binding sites on many of the 3′-UTRs are exceptionally well conserved. This may be due to another role played by these sequences and requires their conservation. miR-298.mr may have evolved its regulation upon these conserved regions and consequently allowed the generation of many targets for this mouse and rat-specific miRNA with no family members.

New miRNA genes may penetrate polycistronic miRNA clusters or preferentially introns of transcribed genes (6). We show that miR-351 is located in a well-conserved miRNA cluster on chromosome X of mice and rats and is transcribed as a polycistron with at least some of the miRNAs in this cluster. All expressed members of this cluster are downregulated following astrocyte activation, implying a transcriptional repression rather than downstream regulation. Thus, miR-351 utilization of an existing transcribed unit, eliminating the need for *de novo* establishment of promoter–enhancer sequences upstream of its gene, has created a favorable hosting environment for this miRNA expression and function.

We chose to compare the miRNA regulatory layer in mice-activated astrocytes to that in common marmoset (*C. jacchus*). Both human and marmoset have closely associated immunity-related genes that are divergent from the mice ones (57). We believe that the overall regulatory layer of miRNAs following astrocyte activation in mice and marmoset follows a similar path. Moreover, the compelling data of the complementary expression of miR-351 and miR-125b in mice and marmoset suggest a parallel role played by these miRNAs in mice and marmoset. This conserved miRNA expression signature has prompted us to study the functionality of the mostly altered miRNAs in our study.

TNF-α is upregulated in a variety of CNS diseases such as brain trauma, ischemic injury, multiple sclerosis and Alzheimer's disease and has been implicated in their pathogenesis (58). We have chosen to focus on the TNF-α signaling pathway, which is consequently affected. This pathway is stimulated in astrocytes by TNF-α secretion from infiltrating peripheral immune cell, microglia and astrocytes themselves, giving rise to autocrine/paracrine stimulation of TNFR1. The FADD/caspase-8 branch of the TNF-α signaling pathway is illustrated in Supplementary Figure 4. miR-155 was previously shown to target the death-domain proteins FADD and RIP, attenuating the TNF-α signaling effect, while it was also shown to increase TNF-α production and subsequently enhance signaling (28), exhibiting a complex regulation for this pathway. We have validated an additional

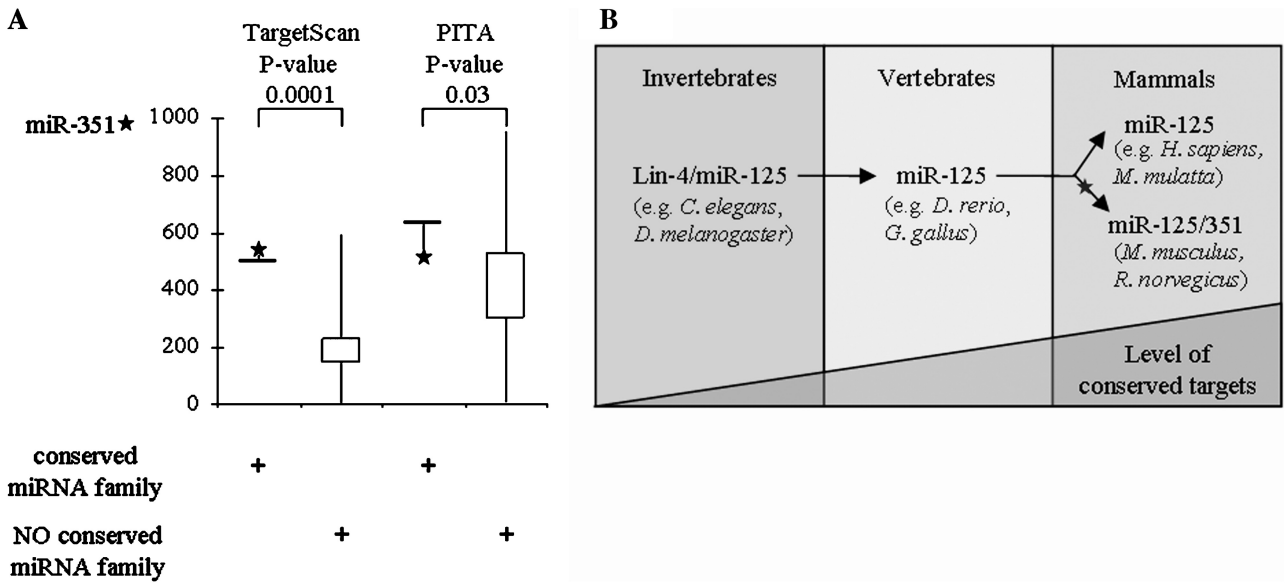

Figure 7. The evolutionary acquisition of miR-351 conserved gene targets. (**A**) A box plot representing the number of conserved binding sites for mouse and rat-specific miRNAs according to two independent target prediction algorithms: TargetScan and PITA (http://genie.weizmann.ac.il/pubs/mir07/mir07_data.html). Intuitively, and not surprisingly, out of these miRNAs, the ones that belong to a well-conserved miRNA family have many more conserved targets (see list of these miRNAs in Supplementary Table S3). (**B**) A simplified representation of miR-125 gene family evolution. miR-125, initially titled lin-4, was first identified in *C. elegans*. miR-351 has probably evolved from one of its family members, somewhere along mice and rats common ancestors (asterisk). Given that all members of miR-125 family possess the same seed region, they are predicted to share the same target genes.

target for miR-155 in this pathway, the death-domain protein, PEA15 which protects astrocytes from TNF-α-induced apoptosis (59).

The 3′-UTR of TNF-α was implicated in its biogenesis (60) long ago. The AU-rich elements (AREs) present in its 3′-UTR were shown to affect TNF-α mRNA stability and the protein translation through miRNAs and miRNA-related proteins (61,62). The TNF-α 3′-UTR possesses conserved miRNA-binding sites outside the AREs and miR-125b was shown to bind one of these (28), allowing the proper production of TNF-α following TLR ligation in macrophages. miR-125 activity was shown to be weak in astrocytes compared to its function in neurons (26). Given that miR-125b and miR-351 share the same targeting specificity (namely, seed region), it did not come as a surprise to find that miR-351 affects the 3′-UTR of TNF-α as well. We show that miR-298.mr also targets this 3′-UTR and in cooperation with miR-351 targets the TNF-α signaling pathway-related SIAH2, as well. By over-expressing or inhibiting miR-351 and miR-298.mr, we further demonstrated that TNF-α and SIAH2 endogenous levels in C6 cells are regulated by both miRNAs. This implies that LPS and IFN-γ-induced astrocyte activation in mice and rats is mediated by miRNAs specific to these species.

Altogether, in this study, we defined a miRNA regulatory signature following astrocyte activation. We identified species-specific miRNAs that play key roles in the control of this process. We revealed that these miRNAs target genes related to the TNF-α signaling pathway. Our study leads to a better understanding of the mechanisms governing astrocyte activation and presents intriguing species-specific miRNAs roles.

SUPPLEMENTARY DATA

Supplementary Data are available at NAR Online.

ACKNOWLEDGEMENTS

The authors thank Prof. Marcello Rosa (Monash University) for providing brain tissue, collected as part of experiments funded by NHMRC project grant 491022 'Plasticity of the primate cerebral cortex'. The authors also thank Prof. Reuven Stein, Lior Mayo and Jakob Rukov for commenting on the article. E.M., Y.C., Y.G., O.E.-S., and N.S. designed research; E.M., Y.C., Y.G., H.Z., S.M., and L.E. performed research; E.M., Y.C., H.Z., O.E.-S., and N.S analyzed data; E.M., O.E.-S., and N.S. wrote the article. This work was performed in partial fulfillment of the requirements for a Ph.D. degree of E.M, Sackler Faculty of Medicine, Tel Aviv University.

FUNDING

Chief Scientist Office, Ministry of Health, Israel (grant No. 3-4876); the Kunz-Lion Foundation; the Ori Levi Foundation for Mitochondrial Research; the Schreiber foundation of Tel Aviv University's Faculty of Medicine; the Wolfson family Charitable Fund; the Legacy Heritage Biomedical Science Partnership Program of the Israel Science Foundation (grant No. 1911/08).

Conflict of interest statement. None declared.

REFERENCES

1. Verkhratski,A.N. and Butt,A. (2007) *Glial Neurobiology: A Textbook*. John Wiley & Sons, Chichester, England a; Hoboken, NJ.
2. Carpentier,P.A., Begolka,W.S., Olson,J.K., Elhofy,A., Karpus,W.J. and Miller,S.D. (2005) Differential activation of astrocytes by innate and adaptive immune stimuli. *Glia*, **49**, 360–374.
3. Buffo,A., Rolando,C. and Ceruti,S. (2009) Astrocytes in the damaged brain: molecular and cellular insights into their reactive response and healing potential. *Biochem. Pharmacol.*, **79**, 77–89.
4. Lewis,B.P., Burge,C.B. and Bartel,D.P. (2005) Conserved seed pairing, often flanked by adenosines, indicates that thousands of human genes are microRNA targets. *Cell*, **120**, 15–20.
5. Kozomara,A. and Griffiths-Jones,S. miRBase: integrating microRNA annotation and deep-sequencing data. *Nucleic Acids Res.*, [Epub ahead of print, 30 October 2010].
6. Shomron,N., Golan,D. and Hornstein,E. (2009) An evolutionary perspective of animal microRNAs and their targets. *J. Biomed. Biotechnol.*, **2009**, 594–738.
7. Chekulaeva,M. and Filipowicz,W. (2009) Mechanisms of miRNA-mediated post-transcriptional regulation in animal cells. *Curr. Opin. Cell. Biol.*, **21**, 452–460.
8. Friedman,R.C., Farh,K.K., Burge,C.B. and Bartel,D.P. (2009) Most mammalian mRNAs are conserved targets of microRNAs. *Genome Res.*, **19**, 92–105.
9. Lim,L.P., Lau,N.C., Garrett-Engele,P., Grimson,A., Schelter,J.M., Castle,J., Bartel,D.P., Linsley,P.S. and Johnson,J.M. (2005) Microarray analysis shows that some microRNAs downregulate large numbers of target mRNAs. *Nature*, **433**, 769–773.
10. Baek,D., Villen,J., Shin,C., Camargo,F.D., Gygi,S.P. and Bartel,D.P. (2008) The impact of microRNAs on protein output. *Nature*, **455**, 64–71.
11. Selbach,M., Schwanhausser,B., Thierfelder,N., Fang,Z., Khanin,R. and Rajewsky,N. (2008) Widespread changes in protein synthesis induced by microRNAs. *Nature*, **455**, 58–63.
12. Bak,M., Silahtaroglu,A., Moller,M., Christensen,M., Rath,M.F., Skryabin,B., Tommerup,N. and Kauppinen,S. (2008) MicroRNA expression in the adult mouse central nervous system. *RNA*, **14**, 432–444.
13. Kosik,K.S. (2006) The neuronal microRNA system. *Nat. Rev. Neurosci.*, **7**, 911–920.
14. Conaco,C., Otto,S., Han,J.J. and Mandel,G. (2006) Reciprocal actions of REST and a microRNA promote neuronal identity. *Proc. Natl Acad. Sci. USA*, **103**, 2422–2427.
15. Sonkoly,E. and Pivarcsi,A. (2009) microRNAs in inflammation. *Int. Rev. Immunol.*, **28**, 535–561.
16. O'Connell,R.M., Rao,D.S., Chaudhuri,A.A. and Baltimore,D. (2010) Physiological and pathological roles for microRNAs in the immune system. *Nat. Rev.*, **10**, 111–122.
17. Junker,A., Krumbholz,M., Eisele,S., Mohan,H., Augstein,F., Bittner,R., Lassmann,H., Wekerle,H., Hohlfeld,R. and Meinl,E. (2009) MicroRNA profiling of multiple sclerosis lesions identifies modulators of the regulatory protein CD47. *Brain*, **132**, 3342–3352.
18. Aronica,E., Fluiter,K., Iyer,A., Zurolo,E., Vreijling,J., van Vliet,E.A., Baayen,J.C. and Gorter,J.A. (2010) Expression pattern of miR-146a, an inflammation-associated microRNA, in experimental and human temporal lobe epilepsy. *Eur. J. Neurosci.*, **31**, 1100–1107.
19. Goldshmit,Y. and Bourne,J. (2010) Upregulation of EphA4 on astrocytes potentially mediates astrocytic gliosis after cortical lesion in the marmoset monkey. *J. Neurotrauma*, **27**, 1321–1332.

20. Benjamini,Y. and Hochberg,Y. (1995) Controlling the false discovery rate: a practical and powerful approach to multiple testing. *J. R. Stati. Soc.*, **57**, 289–300.
21. Voorhoeve,P.M., le Sage,C., Schrier,M., Gillis,A.J., Stoop,H., Nagel,R., Liu,Y.P., van Duijse,J., Drost,J., Griekspoor,A. *et al.* (2006) A genetic screen implicates miRNA-372 and miRNA-373 as oncogenes in testicular germ cell tumors. *Cell*, **124**, 1169–1181.
22. Johann,S., Kampmann,E., Denecke,B., Arnold,S., Kipp,M., Mey,J. and Beyer,C. (2008) Expression of enzymes involved in the prostanoid metabolism by cortical astrocytes after LPS-induced inflammation. *J. Mol. Neurosci.*, **34**, 177–185.
23. Halonen,S.K., Woods,T., McInnerney,K. and Weiss,L.M. (2006) Microarray analysis of IFN-gamma response genes in astrocytes. *J. Neuroimmunol.*, **175**, 19–30.
24. Chung,I.Y. and Benveniste,E.N. (1990) Tumor necrosis factor-alpha production by astrocytes. Induction by lipopolysaccharide, IFN-gamma, and IL-1 beta. *J. Immunol.*, **144**, 2999–3007.
25. Farina,C., Aloisi,F. and Meinl,E. (2007) Astrocytes are active players in cerebral innate immunity. *Trends Immunol.*, **28**, 138–145.
26. Smirnova,L., Grafe,A., Seiler,A., Schumacher,S., Nitsch,R. and Wulczyn,F.G. (2005) Regulation of miRNA expression during neural cell specification. *Eur. J. Neurosci.*, **21**, 1469–1477.
27. Olsen,P.H. and Ambros,V. (1999) The lin-4 regulatory RNA controls developmental timing in *Caenorhabditis elegans* by blocking LIN-14 protein synthesis after the initiation of translation. *Dev. Biol.*, **216**, 671–680.
28. Tili,E., Michaille,J.J., Cimino,A., Costinean,S., Dumitru,C.D., Adair,B., Fabbri,M., Alder,H., Liu,C.G., Calin,G.A. *et al.* (2007) Modulation of miR-155 and miR-125b levels following lipopolysaccharide/TNF-alpha stimulation and their possible roles in regulating the response to endotoxin shock. *J. Immunol.*, **179**, 5082–5089.
29. Saetrom,P., Biesinger,J., Li,S.M., Smith,D., Thomas,L.F., Majzoub,K., Rivas,G.E., Alluin,J., Rossi,J.J., Krontiris,T.G. *et al.* (2009) A risk variant in an miR-125b binding site in BMPR1B is associated with breast cancer pathogenesis. *Cancer Res.*, **69**, 7459–7465.
30. Gefen,N., Binder,V., Zaliova,M., Linka,Y., Morrow,M., Novosel,A., Edry,L., Hertzberg,L., Shomron,N., Williams,O. *et al.* (2009) Hsa-mir-125b-2 is highly expressed in childhood ETV6/RUNX1 (TEL/AML1) leukemias and confers survival advantage to growth inhibitory signals independent of p53. *Leukemia*, **24**, 89–96.
31. Lewis,B.P., Shih,I.H., Jones-Rhoades,M.W., Bartel,D.P. and Burge,C.B. (2003) Prediction of mammalian microRNA targets. *Cell*, **115**, 787–798.
32. Ohler,U., Yekta,S., Lim,L.P., Bartel,D.P. and Burge,C.B. (2004) Patterns of flanking sequence conservation and a characteristic upstream motif for microRNA gene identification. *RNA*, **10**, 1309–1322.
33. Enright,A.J., John,B., Gaul,U., Tuschl,T., Sander,C. and Marks,D.S. (2003) MicroRNA targets in Drosophila. *Genome Biol.*, **5**, R1.
34. Krek,A., Grun,D., Poy,M.N., Wolf,R., Rosenberg,L., Epstein,E.J., MacMenamin,P., da Piedade,I., Gunsalus,K.C., Stoffel,M. *et al.* (2005) Combinatorial microRNA target predictions. *Nat. Genet.*, **37**, 495–500.
35. Didiano,D. and Hobert,O. (2006) Perfect seed pairing is not a generally reliable predictor for miRNA-target interactions. *Nat. Struct. Mol. Biol.*, **13**, 849–851.
36. Dror,N., Alter-Koltunoff,M., Azriel,A., Amariglio,N., Jacob-Hirsch,J., Zeligson,S., Morgenstern,A., Tamura,T., Hauser,H., Rechavi,G. *et al.* (2007) Identification of IRF-8 and IRF-1 target genes in activated macrophages. *Mol. Immunol.*, **44**, 338–346.
37. Han,T.H., Jin,P., Ren,J., Slezak,S., Marincola,F.M. and Stroncek,D.F. (2009) Evaluation of 3 clinical dendritic cell maturation protocols containing lipopolysaccharide and interferon-gamma. *J. Immunother.*, **32**, 399–407.
38. Nakajima,K., Tohyama,Y., Kohsaka,S. and Kurihara,T. (2001) Ability of rat microglia to uptake extracellular glutamate. *Neurosci. Lett.*, **307**, 171–174.
39. Androulidaki,A., Iliopoulos,D., Arranz,A., Doxaki,C., Schworer,S., Zacharioudaki,V., Margioris,A.N., Tsichlis,P.N. and Tsatsanis,C. (2009) The kinase Akt1 controls macrophage response to lipopolysaccharide by regulating microRNAs. *Immunity*, **31**, 220–231.
40. Murphy,A.J., Guyre,P.M. and Pioli,P.A. (2010) Estradiol suppresses NF-kappa B activation through coordinated regulation of let-7a and miR-125b in primary human macrophages. *J. Immunol.*, **184**, 5029–5037.
41. Sonkoly,E., Stahle,M. and Pivarcsi,A. (2008) MicroRNAs: novel regulators in skin inflammation. *Clin. Exp. Dermatol.*, **33**, 312–315.
42. Pogue,A.I., Cui,J.G., Li,Y.Y., Zhao,Y., Culicchia,F. and Lukiw,W.J. (2010) Micro RNA-125b (miRNA-125b) function in astrogliosis and glial cell proliferation. *Neurosci. Lett.*, **476**, 18–22.
43. Renganathan,H., Vaidyanathan,H., Knapinska,A. and Ramos,J.W. (2005) Phosphorylation of PEA-15 switches its binding specificity from ERK/MAPK to FADD. *Biochem. J.*, **390**, 729–735.
44. Sharif,A., Canton,B., Junier,M.P. and Chneiweiss,H. (2003) PEA-15 modulates TNFalpha intracellular signaling in astrocytes. *Ann. NY Acad. Sci.*, **1010**, 43–50.
45. Huang da,W., Sherman,B.T. and Lempicki,R.A. (2009) Systematic and integrative analysis of large gene lists using DAVID bioinformatics resources. *Nat. Protoc.*, **4**, 44–57.
46. Habelhah,H., Frew,I.J., Laine,A., Janes,P.W., Relaix,F., Sassoon,D., Bowtell,D.D. and Ronai,Z. (2002) Stress-induced decrease in TRAF2 stability is mediated by Siah2. *EMBO J.*, **21**, 5756–5765.
47. Barhoumi,R., Faske,J., Liu,X. and Tjalkens,R.B. (2004) Manganese potentiates lipopolysaccharide-induced expression of NOS2 in C6 glioma cells through mitochondrial-dependent activation of nuclear factor kappaB. *Brain Res.*, **122**, 167–179.
48. Gatson,J.W., Simpkins,J.W., Yi,K.D., Idris,A.H., Minei,J.P. and Wigginton,J.G. (2010) Aromatase is increased in astrocytes in the presence of elevated pressure. *Endocrinology*, doi:10.1210/en.2010-0724 [Epub ahead of print, 3 November 2010].
49. Won,J.S., Im,Y.B., Singh,A.K. and Singh,I. (2004) Dual role of cAMP in iNOS expression in glial cells and macrophages is mediated by differential regulation of p38-MAPK/ATF-2 activation and iNOS stability. *Free Radic. Biol. Med.*, **37**, 1834–1844.
50. Pedersen,I.M., Cheng,G., Wieland,S., Volinia,S., Croce,C.M., Chisari,F.V. and David,M. (2007) Interferon modulation of cellular microRNAs as an antiviral mechanism. *Nature*, **449**, 919–922.
51. Liu,D.Z., Tian,Y., Ander,B.P., Xu,H., Stamova,B.S., Zhan,X., Turner,R.J., Jickling,G. and Sharp,F.R. (2010) Brain and blood microRNA expression profiling of ischemic stroke, intracerebral hemorrhage, and kainate seizures. *J. Cereb. Blood Flow Metab.*, **30**, 92–101.
52. Jeyaseelan,K., Lim,K.Y. and Armugam,A. (2008) MicroRNA expression in the blood and brain of rats subjected to transient focal ischemia by middle cerebral artery occlusion. *Stroke Journal of Cerebr. Circ.*, **39**, 959–966.
53. Boissonneault,V., Plante,I., Rivest,S. and Provost,P. (2009) MicroRNA-298 and microRNA-328 regulate expression of mouse beta-amyloid precursor protein-converting enzyme 1. *J. Biol. Chem.*, **284**, 1971–1981.
54. Pan,Y.Z., Gao,W. and Yu,A.M. (2009) MicroRNAs regulate CYP3A4 expression via direct and indirect targeting. *Drug Metab. Dispos.*, **37**, 2112–2117.
55. Farh,K.K., Grimson,A., Jan,C., Lewis,B.P., Johnston,W.K., Lim,L.P., Burge,C.B. and Bartel,D.P. (2005) The widespread impact of mammalian MicroRNAs on mRNA repression and evolution. *Science*, **310**, 1817–1821.
56. Lee,R.C., Feinbaum,R.L. and Ambros,V. (1993) The C. *elegans* heterochronic gene lin-4 encodes small RNAs with antisense complementarity to lin-14. *Cell*, **75**, 843–854.
57. Kohu,K., Yamabe,E., Matsuzawa,A., Onda,D., Suemizu,H., Sasaki,E., Tanioka,Y., Yagita,H., Suzuki,D., Kametani,Y. *et al.* (2008) Comparison of 30 immunity-related genes from the common marmoset with orthologues from human and mouse. *Tohoku J. Exp. Med.*, **215**, 167–180.

58. Akassoglou,K., Douni,E., Bauer,J., Lassmann,H., Kollias,G. and Probert,L. (2003) Exclusive tumor necrosis factor (TNF) signaling by the p75TNF receptor triggers inflammatory ischemia in the CNS of transgenic mice. *Proc. Natl Acad. Sci. USA*, **100**, 709–714.
59. Kitsberg,D., Formstecher,E., Fauquet,M., Kubes,M., Cordier,J., Canton,B., Pan,G., Rolli,M., Glowinski,J. and Chneiweiss,H. (1999) Knock-out of the neural death effector domain protein PEA-15 demonstrates that its expression protects astrocytes from TNFalpha-induced apoptosis. *J. Neurosci.*, **19**, 8244–8251.
60. Jacob,C.O., Lee,S.K. and Strassmann,G. (1996) Mutational analysis of TNF-alpha gene reveals a regulatory role for the 3′-untranslated region in the genetic predisposition to lupus-like autoimmune disease. *J. Immunol.*, **156**, 3043–3050.
61. Jing,Q., Huang,S., Guth,S., Zarubin,T., Motoyama,A., Chen,J., Di Padova,F., Lin,S.C., Gram,H. and Han,J. (2005) Involvement of microRNA in AU-rich element-mediated mRNA instability. *Cell*, **120**, 623–634.
62. Vasudevan,S. and Steitz,J.A. (2007) AU-rich-element-mediated upregulation of translation by FXR1 and Argonaute 2. *Cell*, **128**, 1105–1118.
63. Taganov,K.D., Boldin,M.P., Chang,K.J. and Baltimore,D. (2006) NF-kappaB-dependent induction of microRNA miR-146, an inhibitor targeted to signaling proteins of innate immune responses. *Proc. Natl Acad. Sci. USA*, **103**, 12481–12486.
64. Bazzoni,F., Rossato,M., Fabbri,M., Gaudiosi,D., Mirolo,M., Mori,L., Tamassia,N., Mantovani,A., Cassatella,M.A. and Locati,M. (2009) Induction and regulatory function of miR-9 in human monocytes and neutrophils exposed to proinflammatory signals. *Proc. Natl Acad. Sci. USA*, **106**, 5282–5287.
65. Ruggiero,T., Trabucchi,M., De Santa,F., Zupo,S., Harfe,B.D., McManus,M.T., Rosenfeld,M.G., Briata,P. and Gherzi,R. (2009) LPS induces KH-type splicing regulatory protein-dependent processing of microRNA-155 precursors in macrophages. *FASEB J.*, **23**, 2898–2908.
66. O'Connell,R.M., Taganov,K.D., Boldin,M.P., Cheng,G. and Baltimore,D. (2007) MicroRNA-155 is induced during the macrophage inflammatory response. *Proc. Natl Acad. Sci. USA*, **104**, 1604–1609.
67. Schmidt,W.M., Spiel,A.O., Jilma,B., Wolzt,M. and Muller,M. (2009) In vivo profile of the human leukocyte microRNA response to endotoxemia. *Biochem. Biophys. Res. Commun.*, **380**, 437–441.
68. Liu,G., Friggeri,A., Yang,Y., Park,Y.J., Tsuruta,Y. and Abraham,E. (2009) miR-147, a microRNA that is induced upon Toll-like receptor stimulation, regulates murine macrophage inflammatory responses. *Proc. Natl Acad. Sci. USA*, **106**, 15819–15824.
69. Moschos,S.A., Williams,A.E., Perry,M.M., Birrell,M.A., Belvisi,M.G. and Lindsay,M.A. (2007) Expression profiling *in vivo* demonstrates rapid changes in lung microRNA levels following lipopolysaccharide-induced inflammation but not in the anti-inflammatory action of glucocorticoids. *BMC Genomics*, **8**, 240.